

REPORT DOCUMENTATION PAGE		Form Approved OMB No. 0704-0188	
<small>Public reporting burden for this collection of information is estimated to average 1 hour per response, including the time for reviewing instructions, searching data sources, gathering and maintaining the data needed, and completing and reviewing the collection of information. Send comments regarding this burden estimate or any other aspect of this collection of information, including suggestions for reducing this burden to Washington Headquarters Service, Directorate for Information Operations and Reports, 1215 Jefferson Davis Highway, Suite 1204, Arlington, VA 22202-4302, and to the Office of Management and Budget, Paperwork Reduction Project (0704-0188) Washington, DC 20503.</small> PLEASE DO NOT RETURN YOUR FORM TO THE ABOVE ADDRESS.			
1. REPORT DATE (DD-MM-YYYY) 08-04-2018		2. REPORT TYPE	
4. TITLE AND SUBTITLE Fundamental Degradation Mechanisms of Multi-Functional Nanoengineered Surfaces		3. DATES COVERED (From - To)	
		5a. CONTRACT NUMBER N00014-16-1-2625	
		5b. GRANT NUMBER N00014-16-1-2625	
		5c. PROGRAM ELEMENT NUMBER 1000004633	
6. AUTHOR(S) Nenad Miljkovic		5d. PROJECT NUMBER	
		5e. TASK NUMBER	
		5f. WORK UNIT NUMBER	
7. PERFORMING ORGANIZATION NAME(S) AND ADDRESS(ES) University of Illinois 506 S Wright St, 364 Henry Administration Building Urbana, IL 61801-3620 United States of America		8. PERFORMING ORGANIZATION REPORT NUMBER	
9. SPONSORING/MONITORING AGENCY NAME(S) AND ADDRESS(ES) Office of Naval Research 875 N. Randolph Street Suite 1425 Arlington, VA 22203-1995 United States of America		10. SPONSOR/MONITOR'S ACRONYM(S) ONR	
		11. SPONSORING/MONITORING AGENCY REPORT NUMBER 12049125	
12. DISTRIBUTION AVAILABILITY STATEMENT approved for public release			
13. SUPPLEMENTARY NOTES None			
14. ABSTRACT <p>This project studied multifunctional nanoengineered surfaces to manipulate fluidic and heat transport processes for robust and long-lasting high performance thermal management solutions. More recently, multifunctional nanoengineered surfaces have been developed that can significantly enhance the stability and performance of these systems using thin film evaporation and jumping-droplet condensation. Although proven in lab scale environments, the wide spread utilization of these surfaces has not been successful due to their poor durability. To successfully implement these phase-change based approaches, the first critical step is obtaining the fundamental understanding of the complex degradation mechanisms on such surfaces. This project utilised quantitative experiments and modeling to obtain fundamental insight into the degradation mechanisms underpinning the failure of functional nanoengineered coatings concurrent with vapor-to-liquid phase change. Specifically, the preliminary we identified that functional coating degradation during vapor-to-liquid phase change governs nucleation behavior and must be well understood in order to enhance long-term durability. This project further investigated and systematically studied these phase change mediated dynamics on state-of-the-art functional surfaces, and ultimately extended the understanding and prediction capability to more complex surfaces and other functional coating material systems. The outcomes of the project not only make important contributions to basic science, but also provide a necessary first step to advance the area of high-performance thermal management and enable new capabilities for defense and commercial systems.</p>			

INSTRUCTIONS FOR COMPLETING SF 298

15. SUBJECT TERMS

16. SECURITY CLASSIFICATION OF:

17. LIMITATION OF
ABSTRACT18. NUMBER
OF PAGES

19a. NAME OF RESPONSIBLE PERSON

a. REPORT

b. ABSTRACT

c. THIS PAGE

19b. TELEPHONE NUMBER (*Include area code*)

INSTRUCTIONS FOR COMPLETING SF 298

1. REPORT DATE. Full publication date, including day, month, if available. Must cite at least the year and be Year 2000 compliant, e.g., 30-06-1998; xx-08-1998; xx-xx-1998.

2. REPORT TYPE. State the type of report, such as final, technical, interim, memorandum, master's thesis, progress, quarterly, research, special, group study, etc.

3. DATES COVERED. Indicate the time during which the work was performed and the report was written, e.g., Jun 1997 - Jun 1998; 1-10 Jun 1996; May - Nov 1998; Nov 1998.

4. TITLE. Enter title and subtitle with volume number and part number, if applicable. On classified documents, enter the title classification in parentheses.

5a. CONTRACT NUMBER. Enter all contract numbers as they appear in the report, e.g. F33615-86-C-5169.

5b. GRANT NUMBER. Enter all grant numbers as they appear in the report, e.g. 1F665702D1257.

5c. PROGRAM ELEMENT NUMBER. Enter all program element numbers as they appear in the report, e.g. AFOSR-82-1234.

5d. PROJECT NUMBER. Enter all project numbers as they appear in the report, e.g. 1F665702D1257; ILIR.

5e. TASK NUMBER. Enter all task numbers as they appear in the report, e.g. 05; RF0330201; T4112.

5f. WORK UNIT NUMBER. Enter all work unit numbers as they appear in the report, e.g. 001; AFAPL30480105.

6. AUTHOR(S). Enter name(s) of person(s) responsible for writing the report, performing the research, or credited with the content of the report. The form of entry is the last name, first name, middle initial, and additional qualifiers separated by commas, e.g. Smith, Richard, Jr.

7. PERFORMING ORGANIZATION NAME(S) AND ADDRESS(ES). Self-explanatory.

8. PERFORMING ORGANIZATION REPORT NUMBER. Enter all unique alphanumeric report numbers assigned by the performing organization, e.g. BRL-1234; AFWL-TR-85-4017-Vol-21-PT-2.

9. SPONSORING/MONITORS AGENCY NAME(S) AND ADDRESS(ES). Enter the name and address of the organization(s) financially responsible for and monitoring the work.

10. SPONSOR/MONITOR'S ACRONYM(S). Enter, if available, e.g. BRL, ARDEC, NADC.

11. SPONSOR/MONITOR'S REPORT NUMBER(S). Enter report number as assigned by the sponsoring/ monitoring agency, if available, e.g. BRL-TR-829; -215.

12. DISTRIBUTION/AVAILABILITY STATEMENT. Use agency-mandated availability statements to indicate the public availability or distribution limitations of the report. If additional limitations/restrictions or special markings are indicated, follow agency authorization procedures, e.g. RD/FRD, PROPIN, ITAR, etc. Include copyright information.

13. SUPPLEMENTARY NOTES. Enter information not included elsewhere such as: prepared in cooperation with; translation of; report supersedes; old edition number, etc.

14. ABSTRACT. A brief (approximately 200 words) factual summary of the most significant information.

15. SUBJECT TERMS. Key words or phrases identifying major concepts in the report.

16. SECURITY CLASSIFICATION. Enter security classification in accordance with security classification regulations, e.g. U, C, S, etc. If this form contains classified information, stamp classification level on the top and bottom of this page.

17. LIMITATION OF ABSTRACT. This block must be completed to assign a distribution limitation to the abstract. Enter UU (Unclassified Unlimited) or SAR (Same as Report). An entry in this block is necessary if the abstract is to be limited.

Contract Number: N000141612625

Title: Fundamental Degradation Mechanisms of Multi-Functional Nanoengineered Surfaces

Major Goals:

The main goal of this project is to create multifunctional nanoengineered surfaces to manipulate fluidic and heat transport processes for robust and long-lasting high performance thermal management solutions which utilize both high (water) or low (refrigerant) surface tension fluids. Thermal management is a critical bottleneck for the advancement of a variety of important naval defense systems. Phase-change based microfluidic systems promise compact solutions with high-heat removal capability. However, challenges in implementation lead to poor heat transfer performance in both the evaporator and condenser. More recently, multifunctional nanoengineered surfaces have been developed that can significantly enhance the stability and performance of these systems using thin film evaporation, dropwise and jumping-droplet condensation. Although proven in lab scale environments, the wide spread utilization of these surfaces has not been successful due to their poor durability. To successfully implement these phase-change based approaches, the first critical step is obtaining the fundamental understanding of the complex degradation mechanisms on such surfaces with a range of working fluids having high and low surface tensions.

Accomplishments Under Goals:

Year 1 of the project focused on three main functional surfaces and their degradation mechanisms. First, we observed the formation of high surface energy agglomerates on hydrophobic coatings after condensation/evaporation cycles in ambient conditions. To investigate the deposition dynamics, we studied the agglomerates on fluorine based hydrophobic coatings as a function of condensation/evaporation cycles via optical and scanning electron microscopy, microgoniometric contact angle measurements, nucleation statistics, and energy dispersive X-ray spectroscopy (EDS). While the contact angle did not change, EDS analysis showed the agglomerates to be comprised of mainly carbon, oxygen, and sulfur. The SEM and EDS results indicated that the agglomerates stem from adsorption of volatile organic compounds such as methanethiol (CH_3SH), dimethyl disulfide (CH_3SSCH_3), and dimethyl trisulfide ($\text{CH}_3\text{SSSCH}_3$) on the liquid-vapor interface during water vapor condensation, which act as preferential sites for heterogeneous nucleation after evaporation. The insights gained from this first study elucidate fundamental aspects governing the behavior of both short and long term heterogeneous nucleation on hydrophobic surfaces, suggest previously unexplored microfabrication and air purification techniques, and present insights into the challenges facing the development of durable dropwise condensing surfaces.

In a parallel study, we investigated the fundamental degradation mechanisms of Lubricant-Infused Surfaces (LIS) or Slippery Liquid-Infused Porous Surfaces (SLIPS), which have recently been developed where the defect free slippery surface leads to lesser pinning of water droplets, resulting in their easy removal. Such surfaces enhance rate of condensation of steam, are self-cleaning and self-healing. The remarkable results of LIS with water droplets gives hope of their viability with low surface tension fluids. However the presence of additional liquid in the form of lubricant for LIS brings other issues to consider. We investigated miscibility of such low surface tension fluids with widely used lubricants for designing LIS. We considered a wide range of low surface tension fluids (12 to 48 mN/m) and different categories of lubricants with varied viscosities, namely fluorinated Krytox oils, silicone oils, mineral oil and ionic liquid. We also calculated the cloaking behavior of the lubricants for immiscible pairs of lubricant and the working fluids. We conclude there are very few choices for lubricant selection in designing stable LIS for the low surface tension fluids.

Lastly, using steady state condensation experiments, we show that polymeric functional coatings do not fail due to abrasion or mechanical wear during phase change. The main mechanism of failure is water permeation through the polymeric coating to the high surface energy substrate and mechanical delamination of the coating. This finding will be key to future design considerations of functional coatings for durable and high-performance phase-change heat transfer applications.

Training Opportunities:

The project funded 3 full-time graduate students (not simultaneously). The first student (Patricia Weisensee) has graduated and is currently an Assistant Professor in the Mechanical Engineering Department at the Washington University of Saint Louis. Currently, two students are funded on this project: Alex Wu (Masters) and Hyeongyun Cha (PhD). Alex is planning on remaining for his PhD after obtaining his masters and Hyeongyun is planning on pursuing an academic career in the US after obtaining his doctorate. Due to the heavy experimental nature of the project, both students have received training in surface science characterization techniques at the Material Research Laboratory and Micro-Nano Manufacturing Systems Lab. Examples include: Scanning Probe Microscopy, Scanning Electron Microscopy, Atomic Force Microscopy, Ellipsometry, Time Domain Thermoreflectance, and microfabrication.

Furthermore, both students have developed professionally through the attendance of conferences and professional meetings to present their work stemming from this project. Due to his significant research progress, Hyeongyun Cha has recently received the Mavis Faculty Fellowship, developed in the College of Engineering to facilitate the training of the next generation of great engineering professors. Engineering at Illinois is internationally recognized for the impact of our research and the strength of our graduate education. The doctoral programs that produce this reputation are primarily research-focused and may not provide students interested in academic careers with the opportunity to gain the knowledge of how to become a highly productive faculty member. The fellowship will enable Hyeongyun to participate in a series of workshops, seminars, and activities that cover various aspects of an academic career. Workshop themes include describing life as a faculty member, writing cover letters and CVs, preparing for campus interviews, and defining and achieving success as a faculty member. These workshops are available to all engineering graduate students.

Results Dissemination

The results were disseminated through seminars at invited speaker events by the PI:

- 1) Center of Excellence for Integrated Thermal Management of Aerospace Vehicles, "Tutorial on Nanoengineered Functional Surfaces," Torrance, CA, February 23, 2017.
- 2) British Petroleum, "Nanoengineered Surfaces for Enhanced Energy Transfer," Naperville, IL, February 2, 2017.

And through conference presentations:

- 1) A. Wu, H. Cha, N. Miljkovic, "Droplet Impact Induced Degradation of Hydrophobic Coatings", to be presented at the ASME Summer Heat Transfer Conference, HT2017, Bellevue, WA, July 9-14, 2017.
- 2) A. Wu, N. Miljkovic, "Lubricant-Infused Surface Degradation through Condensation Induced Lubricant Drainage", to be presented at the ASME Summer Heat Transfer Conference, HT2017, Bellevue, WA, July 9-14, 2017.
- 3) A. Wu, N. Miljkovic, "Droplet Cloaking Imaging and Characterization", to be presented at the ASME Summer Heat Transfer Conference, HT2017, Bellevue, WA, July 9-14, 2017.
- 4) H. Cha, M.-K. Kim, J. Yang, A. Wu, N. Miljkovic, "Spontaneous Evaporating Microdroplet Sliding on Hydrophobic Surfaces," to be presented at the ASME Summer Heat Transfer Conference, HT2017, Bellevue, WA, July 9-14, 2017.
- 5) H. Cha, M.-K. Kim, S. Lee, A. Wu, N. Miljkovic, "Agglomerate-Deposition-Mediated Heterogeneous Nucleation during Atmospheric Water Vapor Condensation," to be presented at the ASME Summer Heat Transfer Conference, HT2017, Bellevue, WA, July 9-14, 2017.
- 6) H. Cha, S. Lee, J. M. Chun, N. Miljkovic, "Focal Plane Shift Imaging for the Measurement of Contact Angles," to be presented at the ASME Summer Heat Transfer Conference, HT2017, Bellevue, WA, July 9-14, 2017.
- 7) P. Weisensee, Y. Wang, Q. Hongliang, D. Schultz, W. P. King, N. Miljkovic, "Dropwise Condensation on Lubricant-Infused Surfaces: The Distribution of Droplet Sizes", to be presented at the ASME Summer Heat Transfer Conference, HT2017, Bellevue, WA, July 9-14, 2017.

Plans Next Reporting Period

The main thrusts of year 2 will be the implementation of scanning probe microscopy techniques. Year 1 focused on atmospheric condensation conditions as well as optical microscopy results mainly due to the long lead time for vacuum chamber construction. The three chambers developed are coming online during the summer of 2017 and will be utilized heavily during Year 2 of the project. Although SPM techniques such as

AFM spatial and phase mapping have been used for the studies conducted in Year 1, we would like to transition to CRVM and AFM-IR techniques to gain a better understanding of what is happening to coatings at the nanoscale level.

In addition to more chamber experiments and SPM characterization, the miscibility and cloaking results from Year 1 of the project have redirected our attention away from LIS and SLIPS surfaces and more towards covalently attached liquids which should dramatically reduce condensate drainage. In parallel, the water permeation results have demonstrated that decreasing the water diffusion coefficient through functional surfaces, instead of increasing abrasion resistance, will be the way to achieve long lasting and robust functional surfaces. As such, we will be continuing our collaborations with PPG, Chemours, and Dr. Gozde Ince on developing and testing cross linked iCVD based polymeric coatings with unprecedented water barrier function.

Honors and Awards

- 1) ONR Young Investigator Award
- 2) UK Royal Academy of Engineering Distinguished Visiting Fellowship.

Protocol Activity Status

Distribution Statement:

Approved for public release; distribution is unlimited.

Participants

First Name:	Nenad	Last Name:	Miljkovic
Project Role:	PD/PI		
National Academy Member:	N	Months Worked:	1
Countries of Collaboration			

Agglomerate Formation Results

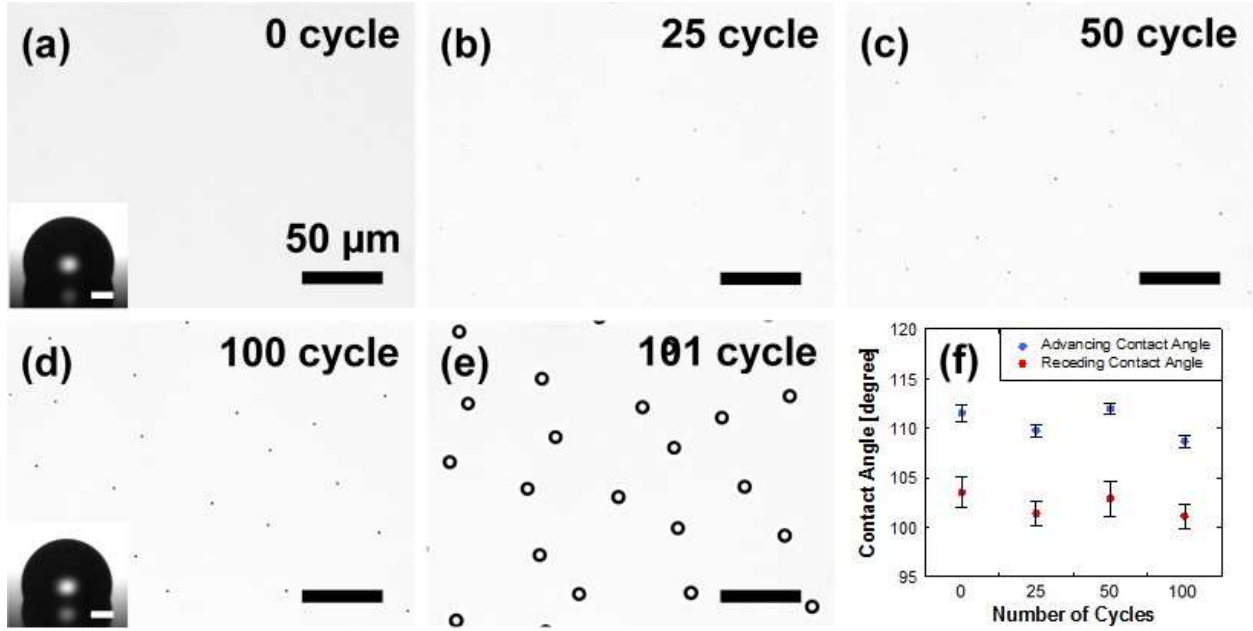


Figure 1. Top-view optical microscopy of agglomerate deposition after (a) 0, (b) 25, (c) 50, and (d) 100 condensation/evaporation cycles on the HTMS coated Si wafer. The deposition and growth of the agglomerates had cycle-dependent size and acted as preferential sites for heterogeneous nucleation as shown in (e). The insets show a microscopic droplet in advancing state on the HTMS coated Si wafer. Inset scale bars are 50 μm each. (f) Advancing and receding contact angles as a function of the number of condensation/evaporation cycles, showing no significant difference in contact angle after condensation/evaporation cycles. A cold stage was used to reduce the sample temperature of $T_w = 1 \pm 0.5^\circ\text{C}$ to induce water droplet condensation and $T_w = 25 \pm 0.5^\circ\text{C}$ to induce evaporation in the laboratory environment condition having an air temperature $T_{\text{air}} = 22 \pm 0.5^\circ\text{C}$ and a relative humidity $\Phi \approx 50 \pm 1\%$.

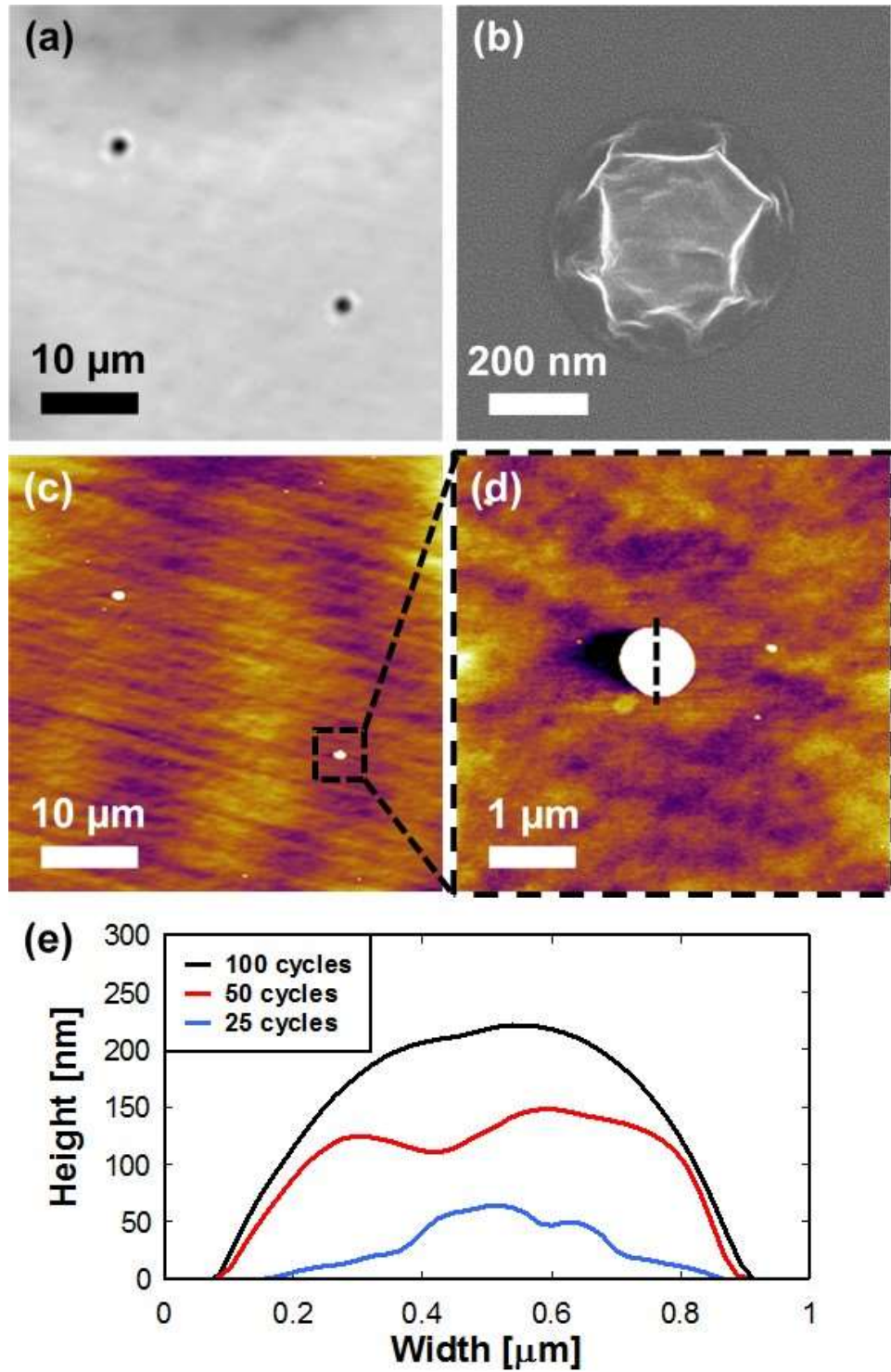


Figure 2. Top-view (a) optical microscopy, (b) field emission scanning electron microscopy, (c) atomic force microscopy (AFM) of agglomerate deposition after 100 condensation/evaporation cycles. (d) High resolution AFM scan of the dotted region in (c). (e) Height profile of individual agglomerates along the black dotted-line trace in (d) as a function of condensation/evaporation cycles.

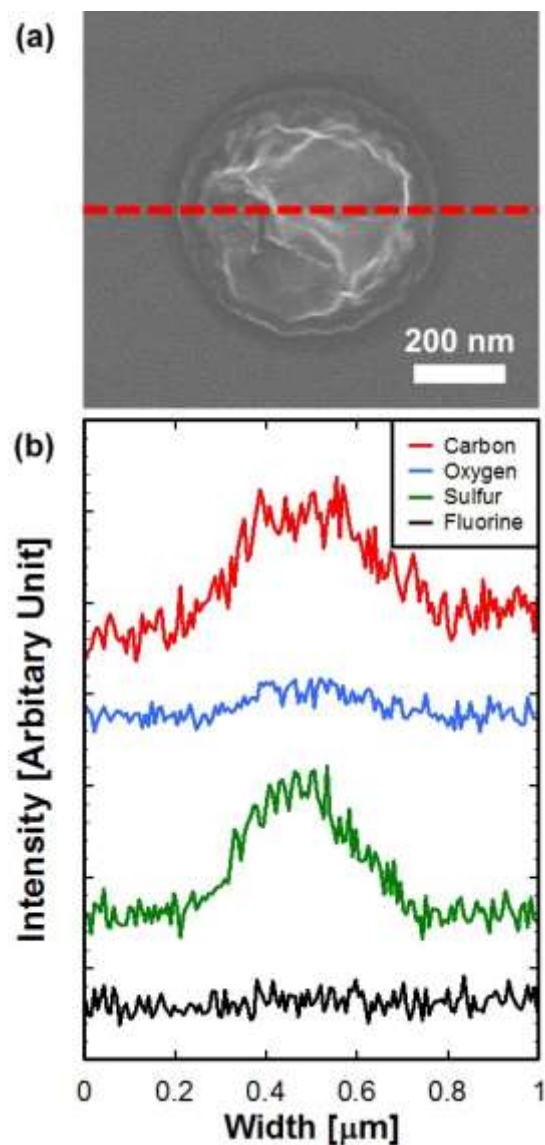


Figure 3. (a) Top-view field emission scanning electron microscopy of agglomerate deposition after 100 condensation/evaporation cycles. (b) Energy dispersive X-ray spectroscopy (EDS) line scans of carbon, oxygen, sulfur, and fluorine along the red dotted-line trace in (a). The results indicate that the agglomerate deposition phenomena is governed by atmospheric sulfur-based hydrocarbon contamination on the liquid-vapor interface composed of carbon, oxygen, and sulfur, not by detachment of fluorine based hydrophobic coating.

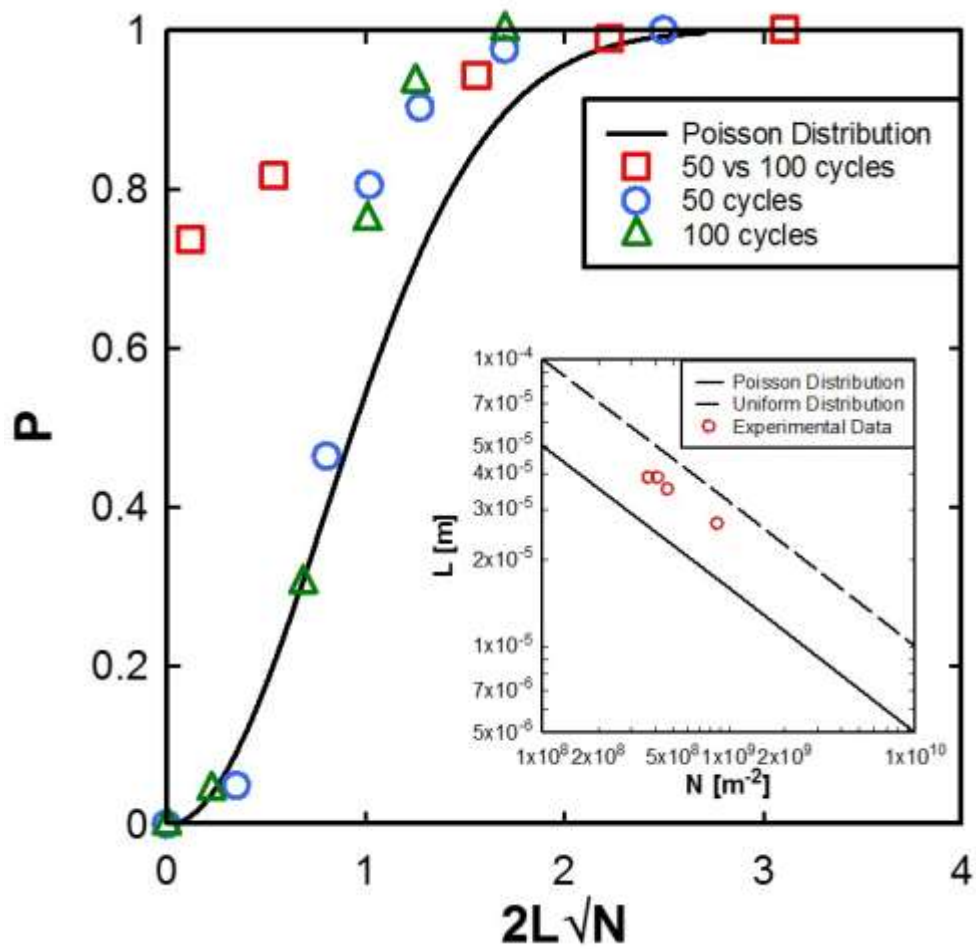


Figure 4. Nucleation behavior on a HTMS coated Si wafer after 50 (blue circle) and 100 (green triangle) condensation/evaporation cycles. Inset: measured mean separation distances. The nucleation sites after 50 and 100 condensation/evaporation cycles were repeatable, as shown by the deviation of the cumulative probability distribution of overlay (red square) of 50 and 100 condensation/evaporation cycles from the predicted Poisson distribution, $P = 1 - \exp(-N\pi L^2)$.

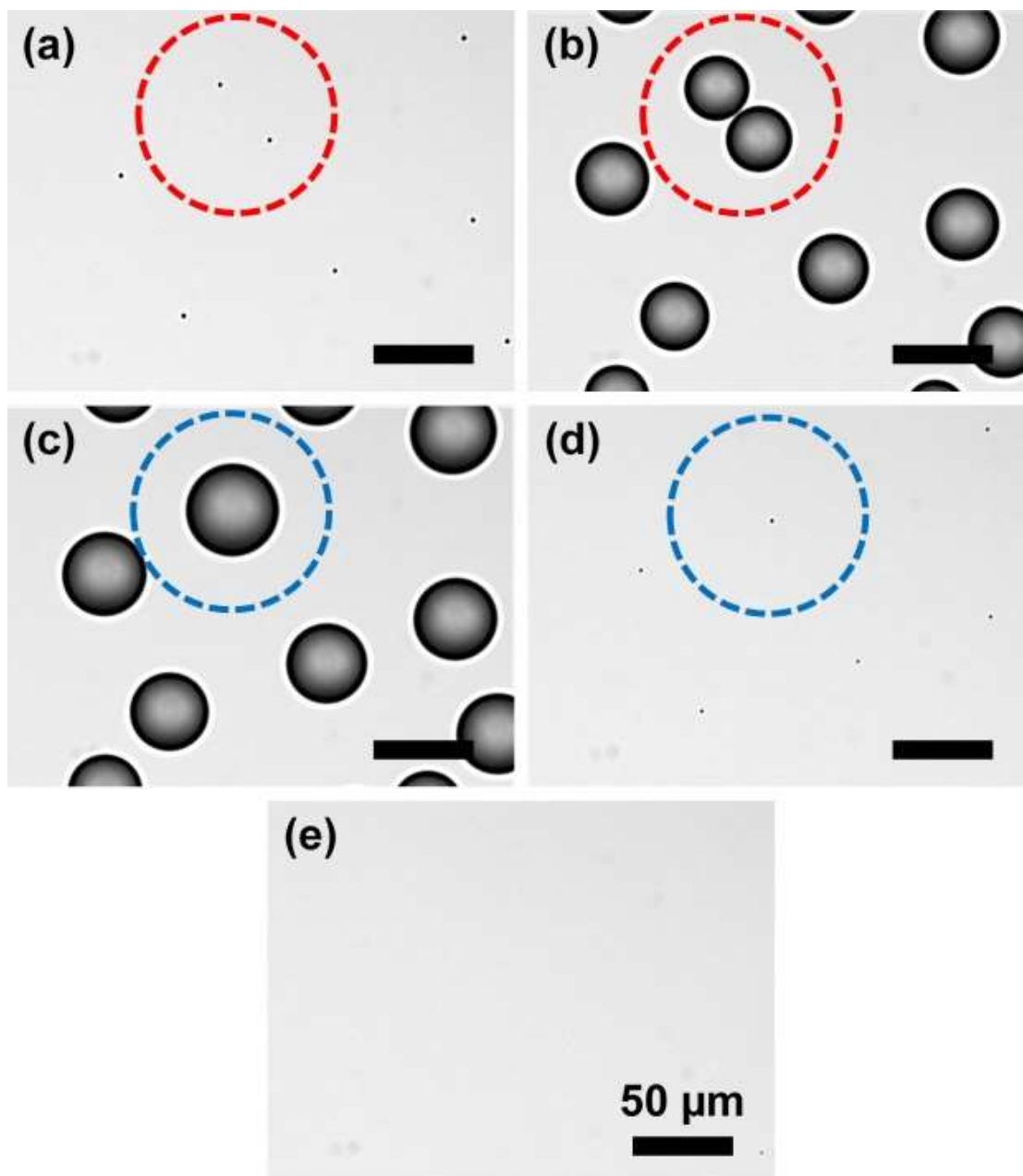


Figure 5. Top-view optical microscopy of the: (a) distribution of agglomerates on the surface after 25 condensation/evaporation cycles, and (b) water droplet condensation during the 26th cycle showing preferential heterogeneous nucleation on the agglomerates, (c) coalescence of condensing water droplets, and (d) subsequent evaporation showing that water droplet coalescence also resulted in the coalescence of agglomerates. The coalescence of agglomerates indicate either agglomerate molecule solubility inside condensate droplets or self-assembly on the liquid-vapor interface. Red and blue dotted-circle indicate the agglomerate and water droplet before and after coalescence, respectively. (e) Surface after cleaning with DI water showing removal of all agglomerates.

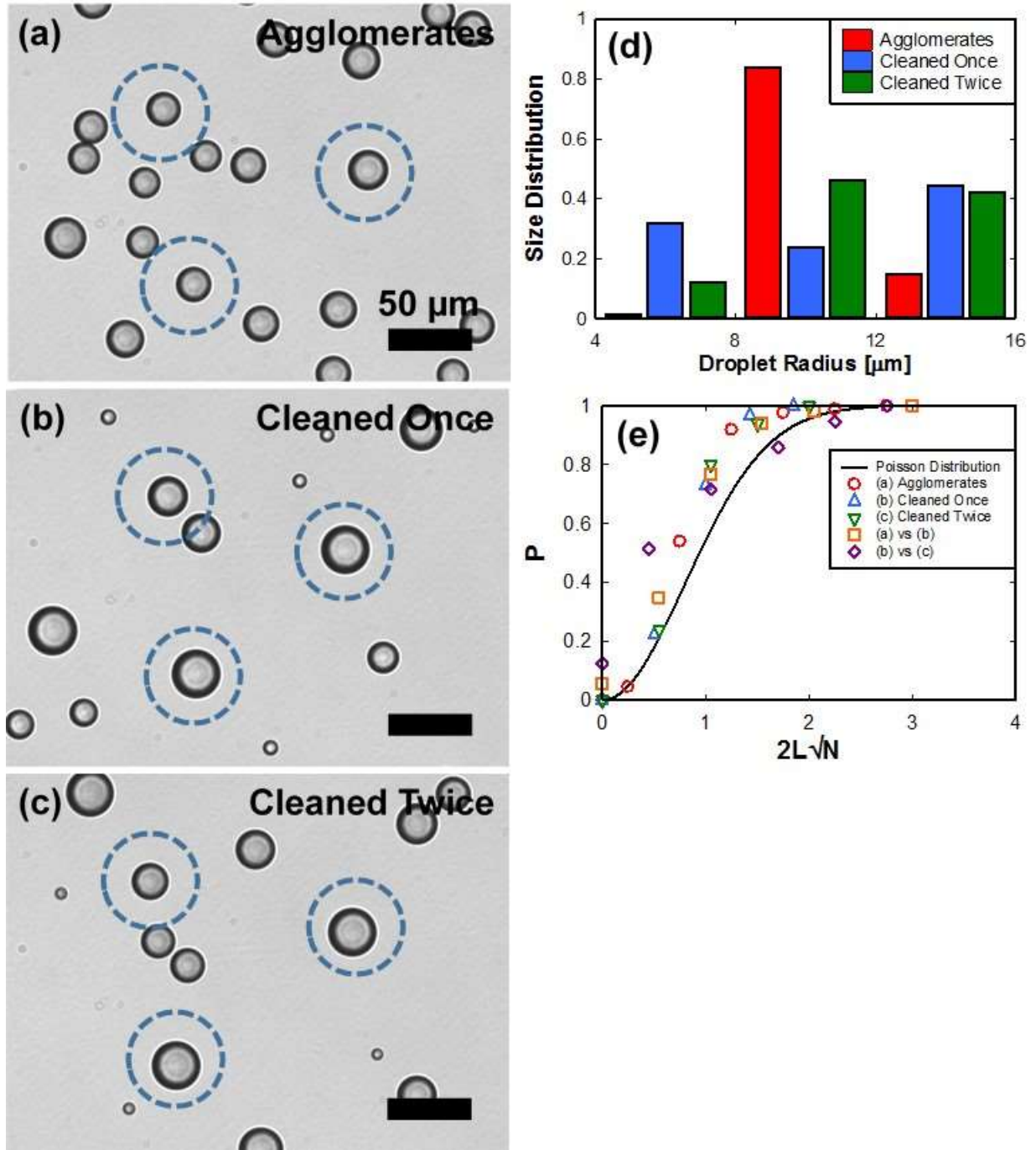


Figure 6. Top-view optical microscopy of water droplet condensation (a) on agglomerate deposited surface, (b) on first-cleaned surface, and (c) on second-cleaned surface. (c) Droplet size distribution for agglomerate deposited surface and cleaned surface. Blue dotted-circle indicate possible defects sites where the nucleation repeats on identical location. Nucleation initiates uniformly on the agglomerates due to high surface energy of agglomerates, while nucleation initiates consecutively on a cleaned surface. (d) Nucleation behavior, showing that nucleation sites are not repeatable after cleaning the agglomerates.

SLIPS Durability Results

Table 1. Physical properties of the tested lubricants and low surface tension fluids at 20°C.

Lubricant	Liquid Density, ρ [kg/m³]	Liquid-Vapor Surface Tension, γ [mN/m]	Vapor Pressure, P_{vap} [kPa]	Dynamic Viscosity, μ [mPa·s]
Krytox – 1506	1880	17	5×10^{-8}	113
Krytox – 1525	1900	19	1.3×10^{-8}	496
Krytox – 16256	1920	19	4×10^{-15}	5216
Carnation Oil	810	28	10^{-2}	9.7
Silicone Oil SO – 5	918	19	0.7	4.6
Silicone Oil SO – 100	970	21	0.7	97
Silicone Oil SO – 500	971	21	0.7	486
Silicone Oil SO - 1000	971	21	0.7	971
Ionic liquid BMIm	1430	34	Not Available	64
Working Fluid				
Water	1000	72.7	2.33	0.89
Ethylene glycol	1113	48.4	7.5×10^{-3}	16.2
Ethanol	789	24.8	5.83	1.095
Isopropanol	786	21.4	4.4	2.38
Pentane	626	15.1	57.9	0.24
Hexane	655	18	16.2	0.297
Toluene	867	27.9	2.93	0.55
Perfluorohexane	1680	12	25	0.64

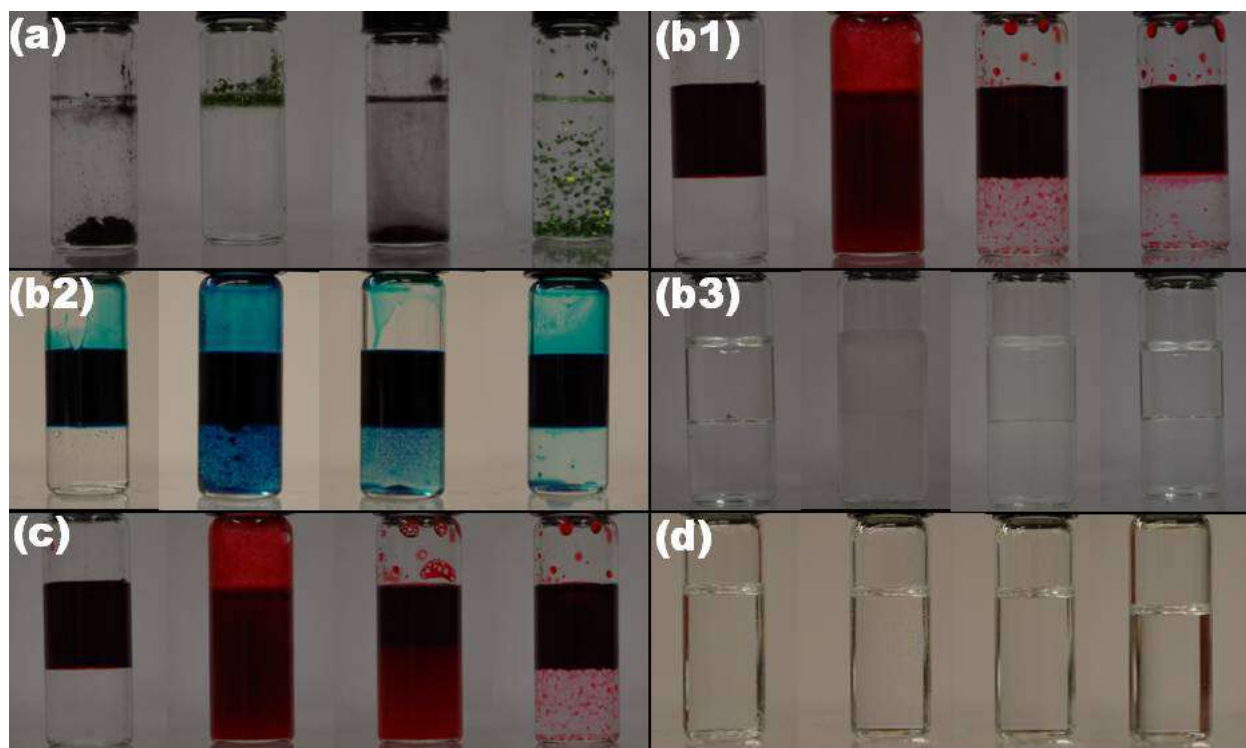


Figure 1. Optical images of the miscibility tests of lubricants with different low surface tension fluids. (a) Insolubility of the dyes used with lubricants – Pylakor Deep Red in Krytox 1525, Brilliant Green in Krytox 1525, Pylakor Deep Red in Silicone oil – 500, and Brilliant Green in Silicone oil – 500. Immiscibility of (b) water, (c) ethanol, and (d) hexane with lubricant Krytox 1525. The difference in viscosity enabled the visualization of the lubricant and working fluid separately for cases with no dye. Lubricant Krytox 1525 with (e) partially miscible ethylene glycol, and (f) completely miscible hexane. In figures (b) – (f), the four different snapshots correspond to the two liquids before mixing, just after mixing, 5 min after mixing and 1 h after mixing, respectively.

Table 2. Miscibility test results. Green corresponds to immiscible (I), yellow corresponds to partially miscible (PM) and red corresponds to completely miscible (M) liquids. Isopropanol is labeled as IPA.

	Water	Ethylene Glycol	Ethanol	IPA	Pentane	Hexane	Toluene	Perfluoro-hexane
Krytox 1506	I	PM	I	I	I	I	I	M
Krytox 1525	I	PM	I	I	I	I	I	M
Krytox 16256	I	I	I	I	I	I	I	M
Carnation	I	I	I	M	M	M	M	I
SO – 5	PM	PM	M	M	M	M	M	I
SO – 100	I	PM	PM	M	M	M	M	I
SO – 500	I	PM	PM	M	M	M	M	I
SO – 1000	I	PM	PM	M	M	M	M	I
BMIm	I	M	M	M	I	I	M	I

Table 3. Spreading coefficient, S_{ol} of lubricants on the working fluids calculated using vOCG method, where n/a corresponds to miscible liquids (Table 2). Note, due to unavailability of the polar surface tension components, calculations could not be performed for lubricant BMIm with the working fluids. Isopropanol is labeled as IPA. Green shading corresponds to cloaking ($S_{ol} > 0$) and red shading corresponds to non-cloaking ($S_{ol} < 0$). Isopropanol is labeled as IPA.

	Water	Ethylene Glycol	Ethanol	IPA	Pentane	Hexane	Toluene	Perfluoro-hexane
Krytox 1506	4.502	10.407	1.180	1.76	-5.079	-0.964	1.372	n/a
Krytox 1525	2.704	8.947	-0.809	-0.2	-7.426	-3.074	-0.605	n/a
Krytox 16256	2.704	8.947	-0.809	-0.2	-7.426	-3.074	-0.605	n/a
Carnation	-6.587	0.991	-10.851	n/a	n/a	n/a	n/a	0.498
SO - 5	2.047	8.404	n/a	n/a	n/a	n/a	n/a	7.990
SO - 100	0.891	7.438	-2.793	n/a	n/a	n/a	n/a	7.012
SO - 500	0.694	7.273	-3.007	n/a	n/a	n/a	n/a	6.845
SO - 1000	0.596	7.190	-3.114	n/a	n/a	n/a	n/a	6.761
BMIm	-	-	-	-	-	-	-	-

Table 4. Spreading coefficient, S_{ol} of the lubricants on the working fluids calculated from measured interfacial tension between the two fluids using the pendant drop method, where n/a corresponds to miscible liquids (Table 2). Green shading corresponds to cloaking ($S_{ol} > 0$) and red shading corresponds to non-cloaking ($S_{ol} < 0$). Due to the low surface tension of perfluorohexane and vanishing interfacial tension with the lubricants, measurements were not possible using the pendant drop method. Isopropanol is labeled as IPA.

	Water	Ethylene Glycol	Ethanol	IPA	Pentane	Hexane	Toluene	Perfluoro-hexane
Krytox 1506	3.643	6.439	-3.702	2.85	-4.282	-1.216	5.422	n/a
Krytox 1525	3.185	6.310	-4.106	-1.72	-5.478	-2.547	1.046	n/a
Krytox 16256	3.271	7.279	-4.832	-2.16	-5.830	-2.450	1.634	n/a
Carnation	-5.664	3.125	-8.324	n/a	n/a	n/a	n/a	-
SO – 5	3.114	7.429	n/a	n/a	n/a	n/a	n/a	-
SO – 100	2.947	7.816	-1.646	n/a	n/a	n/a	n/a	-
SO – 500	3.016	8.452	-2.014	n/a	n/a	n/a	n/a	-
SO – 1000	2.518	8.063	-1.983	n/a	n/a	n/a	n/a	-
BMIm	-4.760	n/a	n/a	n/a	-24.127	-20.863	n/a	-

Table 5. Combined miscibility and cloaking results. Green cells labeled PASS correspond to immiscible and non-cloaking lubricant-fluid pairs, and red cells labeled FAIL corresponds to either miscible, or cloaking, or both lubricant-fluid pairs. Isopropanol is labeled as IPA.

	Water	Ethylene Glycol	Ethanol	IPA	Pentane	Hexane	Toluene	Perfluoro-hexane
Krytox 1506	FAIL	FAIL	PASS	FAIL	PASS	PASS	FAIL	FAIL
Krytox 1525	FAIL	FAIL	PASS	PASS	PASS	PASS	FAIL	FAIL
Krytox 16256	FAIL	FAIL	PASS	PASS	PASS	PASS	FAIL	FAIL
Carnation	PASS	FAIL	PASS	FAIL	FAIL	FAIL	FAIL	FAIL
SO - 5	FAIL	FAIL	FAIL	FAIL	FAIL	FAIL	FAIL	FAIL
SO - 100	FAIL	FAIL	PASS	FAIL	FAIL	FAIL	FAIL	FAIL
SO - 500	FAIL	FAIL	PASS	FAIL	FAIL	FAIL	FAIL	FAIL
SO - 1000	FAIL	FAIL	PASS	FAIL	FAIL	FAIL	FAIL	FAIL
BMIm	PASS	FAIL	FAIL	FAIL	PASS	PASS	FAIL	